# Supporting Information For:

## Multiple Epsilon-Near-Zero Resonances in Multilayered Cadmium Oxide: Designing Metamaterial-like Optical Properties in Monolithic Materials

Kyle P. Kelley[1], Evan L. Runnerstrom[1,*], Edward Sachet[1], Christopher T. Shelton[1], Everett D. Grimley[1], Andrew Klump[1], James M. LeBeau[1], Zlatko Sitar[1], Jonathan Y. Suen[2], Willie J. Padilla[2], and Jon-Paul Maria[1,3,*]

[1] Department of Materials Science and Engineering, North Carolina State University, Raleigh, NC 27695

[2] Department of Electrical and Computer Engineering, Duke University, Durham, NC 27708

[3] Department of Materials Science and Engineering, The Pennsylvania State University, University Park, PA 16802

* To whom correspondence may be addressed: elrunner@ncsu.edu; jpm133@psu.edu

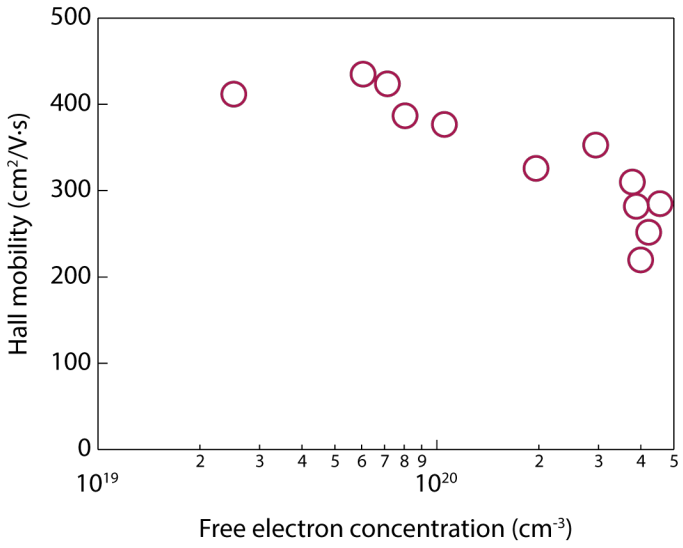


**Figure S1:** Mobility vs. free carrier concentration (measured by Hall effect) for In:CdO thin films grown on *r*-plane sapphire.

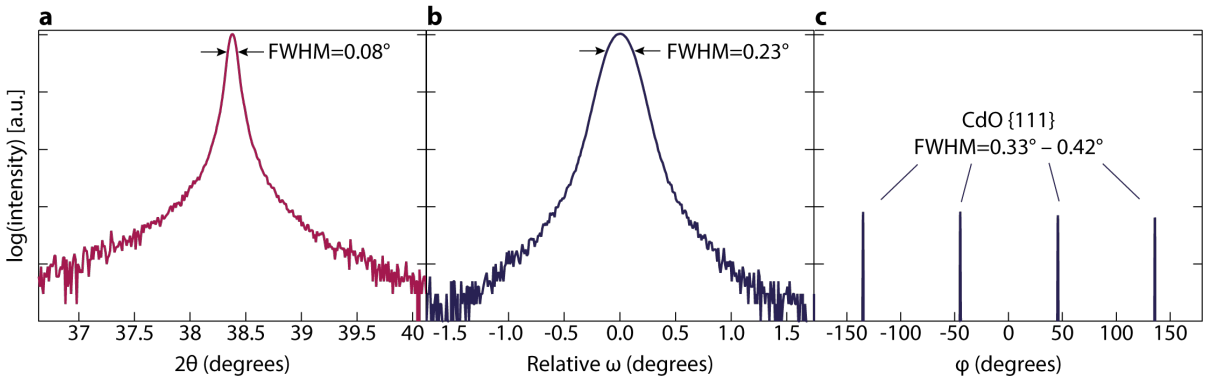


**Figure S2:** High-resolution X-ray diffraction analysis of three-layered stack (same intensity scale for all three panels). (a) CdO (002) diffraction peak. (b) Rocking curve about the CdO (002) peak. (c) Skew-symmetric ϕ-scan about the CdO (111) peak (χ: 54.7°, 2θ:33.0°). The four-fold symmetry shows indicates a single epitaxial relationship between all three CdO layers and the substrate.

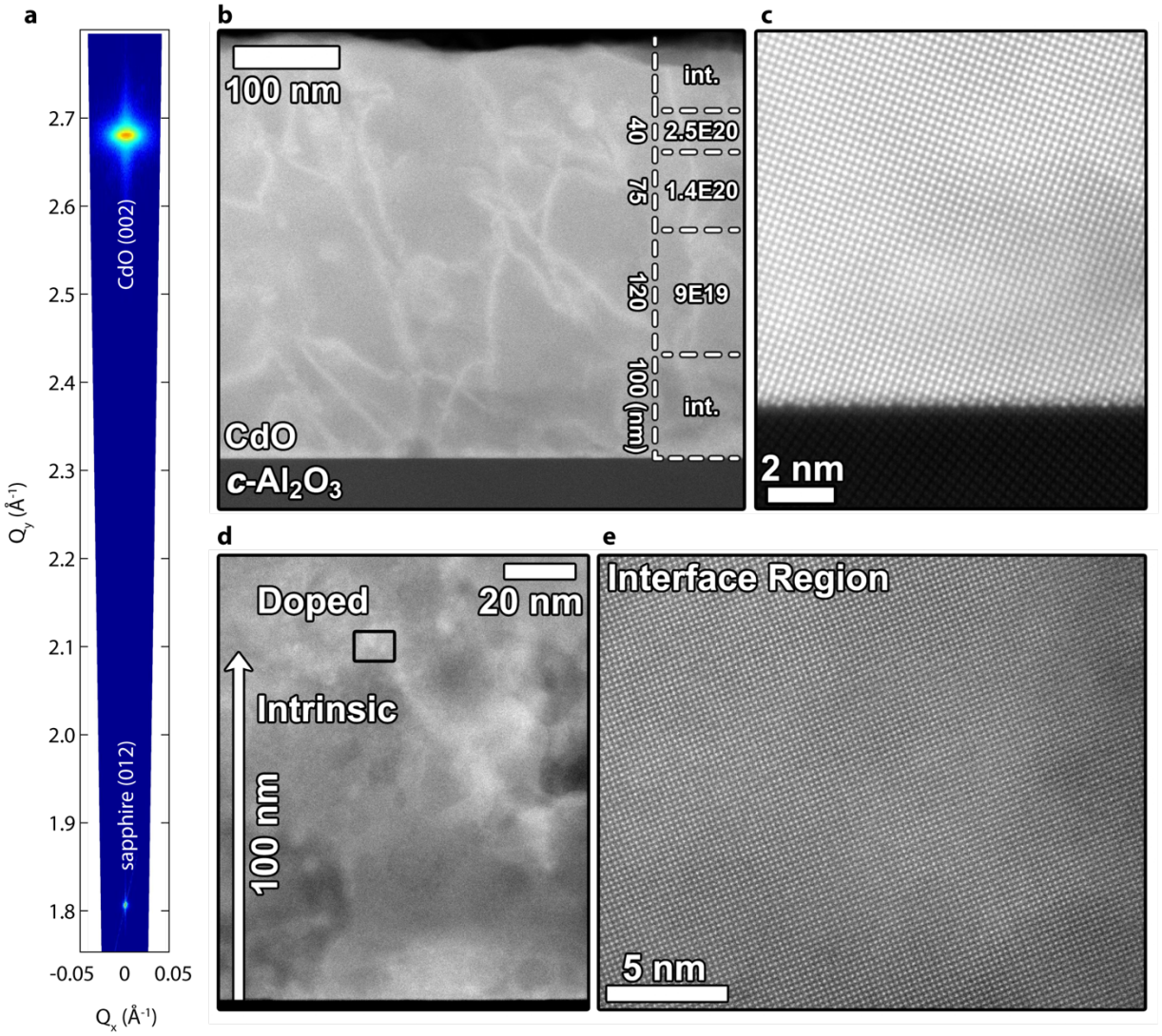


**Figure S3:** (a) Reciprocal space map of the three-layer stack collected using XRD. The single CdO (002) peak orientation indicates a single epitaxial relationship between all three CdO layers and the *r*-plane sapphire substrate. (b) Scanning transmission electron microscopy (STEM) of a representative three-ENZ layered stack sandwiched between two undoped CdO layers, deposited on *c*-plane sapphire. The thickness and carrier concentration (in $cm^{-3}$) of each layer is overlaid on the right side of the image. (c) STEM image showing epitaxy between the CdO and the substrate. (d-e) STEM images in the vicinity of an interface between the bottom undoped layer and the first ENZ layer (atomic resolution image in panel e is from the black box inset in panel d). Note the absence of any discernible physical interfaces between adjacent CdO layers. Note: *c*-plane sapphire was chosen as the substrate for STEM imaging because of the ease of sample preparation and high-quality imaging.

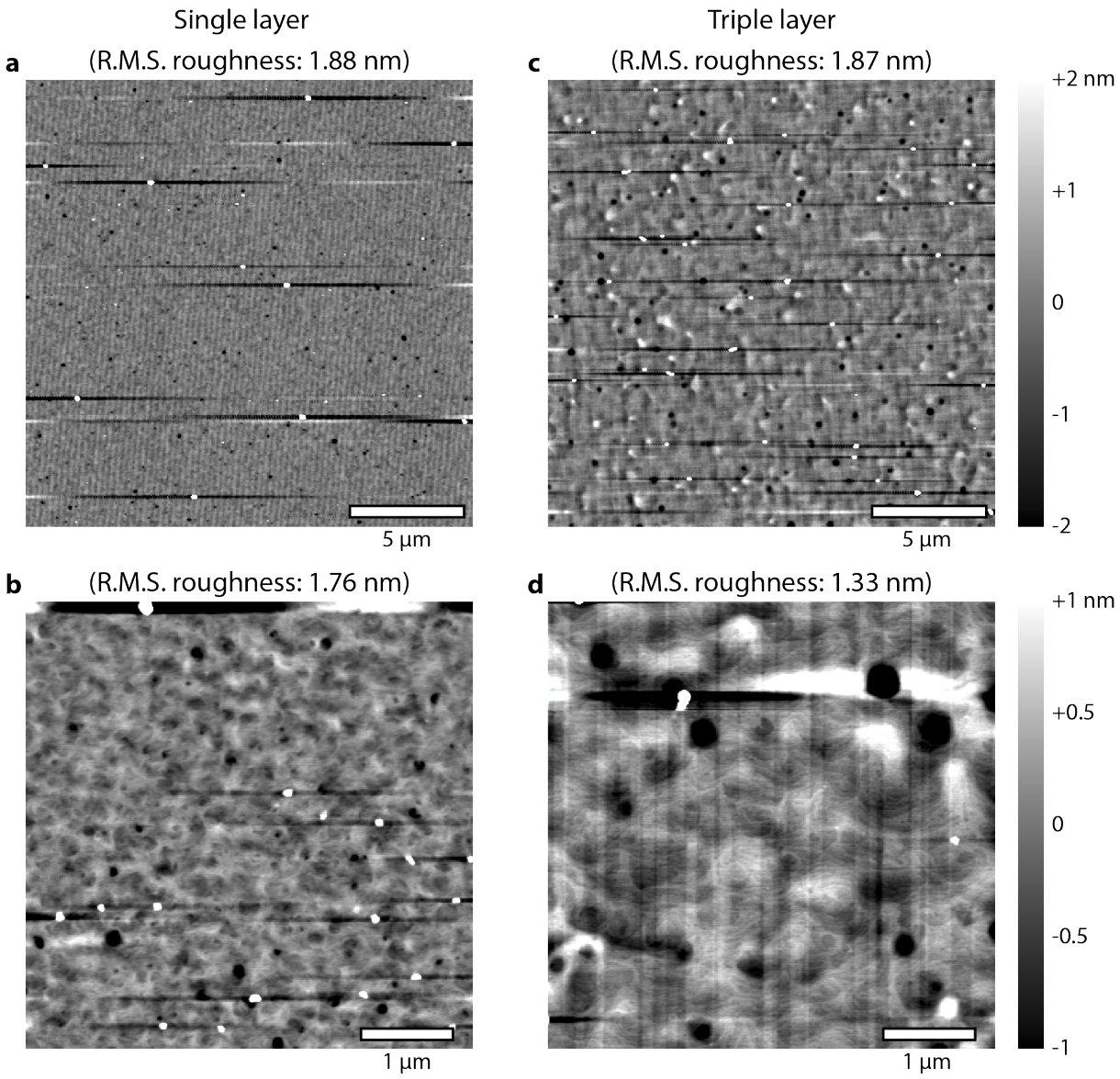


**Figure S4:** Atomic force microscopy (AFM) images of single-layer (a – b) and three-layer (c – d) In:CdO surfaces. The noted root mean square (R.M.S.) roughness is taken for each entire image (including particle contamination).

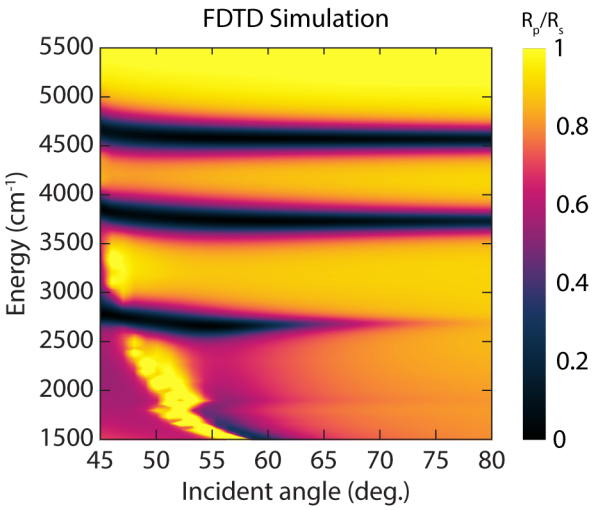


**Figure S5:** Infrared reflectivity map ($R_p/R_s$) of the three-layer stack as simulated by the finite difference time domain method (Lumerical FDTD). (Kretschmann configuration).

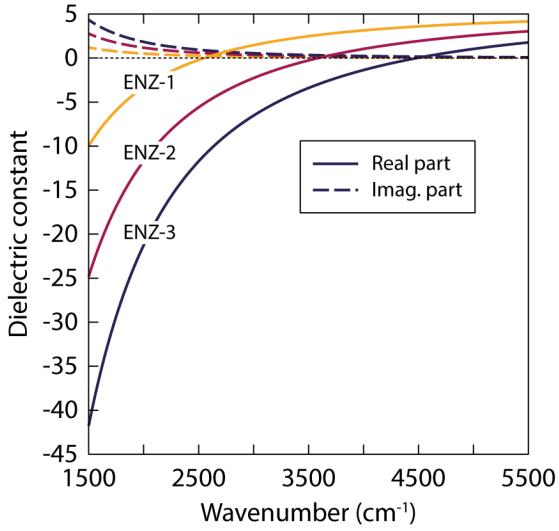


**Figure S6:** Simulated dielectric functions (Drude model) of each ENZ layer in the three-layer stack.

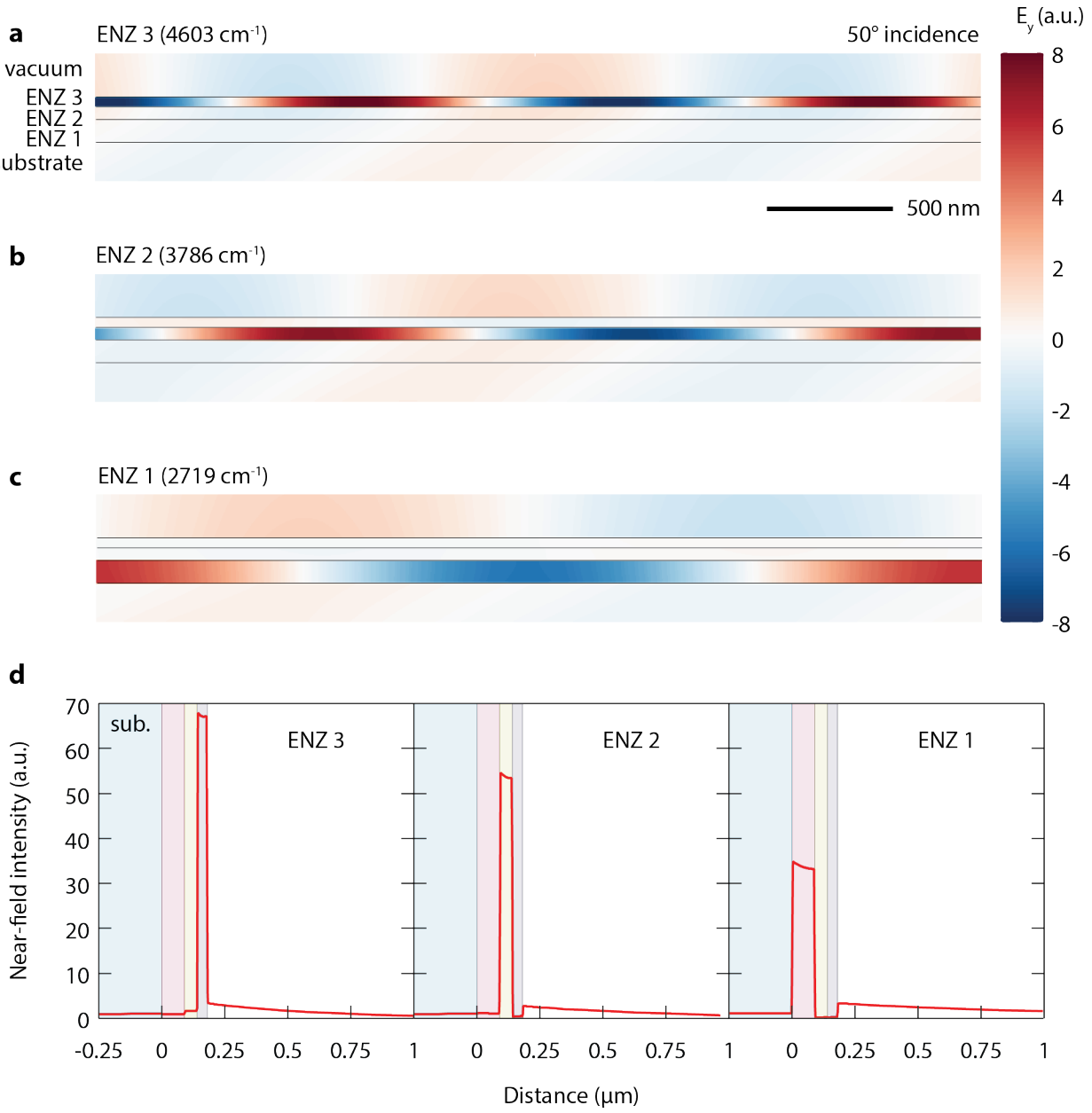


**Figure S7:** Near-field mode profiles of the three individual resonant ENZ modes in the three-layer stack. The incident light electric field intensity is defined as 1 and the incident angle (Kretschmann configuration) is 50°. See Figure 3c in the main text for the FDTD-simulated infrared reflectivity spectrum of the three-layer stack at 50°. (a) Mode profile of the high-energy absorption peak at ~4600 $cm^{-1}$, corresponding to the ENZ frequency of the top CdO layer (ENZ 3). (b) Mode profile of the medium-energy absorption peak at ~ 3800 $cm^{-1}$ (middle layer, ENZ 2). (c) Mode profile of the low-energy absorption peak at ~2700 $cm^{-1}$ (bottom layer, ENZ 1). (d) One-dimensional electric field intensity profiles through the thickness of the film. Note that the electric field is almost entirely confined within its respective ENZ layer, with a small evanescent decay into the surrounding medium.

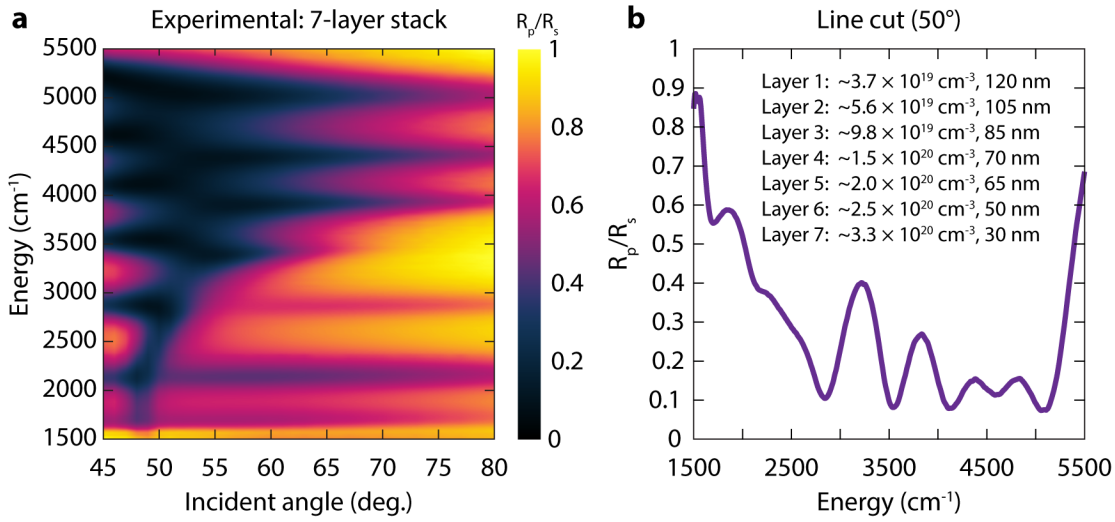


**Figure S8:** Example of a monolithic, broadband plasmonic absorber comprised of 7 In:CdO ENZ layers. (a) Experimental reflectivity map (Kretschmann configuration) of the 7 layer stack. (b) Line cut of the reflectivity at 50° incident angle. The approximate carrier concentration and thickness of each layer is given in the inset of panel (b).

**Additional experimental details:**

*Film/multilayer growth*: In:CdO thin films and multilayers were deposited using reactive high-power impulse magnetron sputtering (R-HiPIMS) from metallic Cd (99.9999%, Osaka Asahi Metal) pressed into a 2-inch target and mounted to MeiVac MAK sputtering source. The HiPIMS pulsing parameters were kept constant at: 80 μs pulse length, 800 Hz repetition rate, and 400 V applied voltage. This corresponds to a 1250 μs period and 6.4% duty cycle, with a time-averaged DC current of 80 mA and a time-averaged DC power of 32 W. This led to a deposition rate of approximately 23 nm/min, as measured by X-ray reflectivity (XRR). DC power was supplied by an Advanced Energy MDX 1.5K DC power supply, and the pulses were generated by a Starfire Industries Impulse Pulsed Power Module.

Doping was achieved by RF (13.56 MHz) co-sputtering from metallic In (99.9999% metal basis, Indium Corporation) pressed into a 2-inch target and mounted to MeiVac MAK sputtering source. Changes in doping level were achieved by changing the RF power applied to the In target. RF power was supplied by an Advanced Energy RFX-600 with a Manitou Systems manual matching network. Small changes to the overall deposition rate with different applied RF power were consistent and reproducible as measured by XRR. All depositions occurred at an operating

pressure of 10 mTorr, maintained by flowing 20 sccm Ar and 14 sccm $O_2$ and by partially closing a gate valve in front of the vacuum system's turbomolecular pump.

To fabricate multilayered samples, each layer was deposited for a specific time and with a specific RF power applied to the In target in order to produce a layer with a target thickness and carrier concentration. These thicknesses and carrier concentrations were calibrated using XRR and Hall effect measurements, respectively. In between each layer, the sample shutter was closed for 2 minutes while the RF power was adjusted to the target value.

Films and multilayers were generally grown on double-polished epi-ready *r*-plane sapphire substrates (Jiaozuo TreTrt Materials) bonded to a stainless-steel puck using silver paint (Ted Pella). The samples for thermal emission measurements were grown on Pt-coated *c*-plane sapphire substrates. (The 100 nm-thick Pt layer was deposited by 10W RF sputtering from a 1-inch Pt target at 5 mTorr Ar and 400°C substrate temperature.) For all CdO depositions, the puck surface temperature was 370°C as monitored by a Raytek 1.6μm MM Series Pyrometer. After deposition, all In:CdO samples annealed at 700°C for 30 minutes in 1 atmosphere static oxygen (99.6%).

*Characterization*: In:CdO transport properties were measured using an Ecopia HMS-3000 Hall measurement system with a 0.51 T magnet using the Van der Pauw method. Thickness was measured by X-ray reflectivity (XRR), and high-resolution X-ray diffraction (XRD) was performed using a PANalytical Empyrean XRD with an incident double bounce hybrid monochromator beam optic and parallel plate collimator (0.18° acceptance angle) diffracted beam optic. Reciprocal space maps were collected using a PANalytical PIXcel area detector.

ToF-SIMS analyses were performed using an ION-TOF TOF-SIMS V instrument with a cesium source for sputtering and a bismuth liquid metal ion gun (LMIG) source in interlaced sputtering mode for analysis. For the depth profiles, a $Cs^+$ beam with 1 keV energy and 8 nA current was rastered over a 120 × 120 μm area. The $Bi_3^+$ beam was 0.4 pA at 25 keV and rastered over a 50 × 50 μm area at the center of the sputtered crater. The angle of incidence was 45° from normal for both beams.

Reflectivity data were obtained using a Woollam infrared variable-angle spectroscopic ellipsometer (IR-VASE) with a custom-built aluminum sample stage to access the Kretschmann-Raether configuration. A 90° calcium fluoride ($CaF_2$) prism was used to couple IR light into the

plasmonically active samples. To ensure good optical contact between the substrate and prism, 1.720 index-matching fluid was used (Cargille Series M).

Thermal emission spectra of In:CdO thin films and multilayers were collected using a Bruker Vertex 80v Fourier-transform infrared spectrometer under vacuum. The samples were mounted on an external rotation stage heated to 400°C using a brass plate with a square-cut opening, and light was collected through a KBr window into the internal beam path of the spectrometer. Emission spectra were collected over multiple angles ranging from 0° (normal incidence) to 80°. Because of the brass plate with the finite opening, the spectra were normalized by the projected area of the sample onto the KBr window (i.e., $1/\cos\theta$) at each angle. The emissivity values were calculated by subtracting the background emission spectra of the stage + blank Pt-coated substrate at each angle, and by dividing the blackbody radiation spectrum at each angle. The reference blackbody spectra at each angle were collected from a Si substrate covered with lampblack film.

*Simulation*: Simulated reflectivity maps were generated from a multilayer transfer-matrix algorithm employing a modified Nelder-Mead simplex optimization, coded in MATLAB. A lossy Drude-based model (Equation 1) was used to simulate the free electron plasma-like IR dielectric function of In:CdO, using an effective mass of 0.21 and a high frequency dielectric constant of 5.3. The dispersion relationship for a 90° calcium fluoride prism and sapphire substrate used for the Kretschmann-Raether configuration is included in the transfer-matrix algorithm to match the experimental setup.

Reflectivity spectra and electric field profiles were additionally simulated using commercial finite-difference time-domain (FDTD) software from Lumerical. The simulation consisted of a sapphire substrate and In:CdO multilayers as detailed in Table 1 of the main text. Plane waves (amplitude of 1) were excited at calculated angles within the sapphire substrate to emulate the Kretschmann configuration.